

First-principle calculation of $\eta_c \rightarrow 2\gamma$ decay width from lattice QCD

Yu Meng,^{1,2} Xu Feng,^{1,2,3} Chuan Liu,^{1,2,3} Teng Wang,¹ and Zuoheng Zou¹

¹*School of Physics, Peking University, Beijing 100871, China*

²*Center for High Energy Physics, Peking University, Beijing 100871, China*

³*Collaborative Innovation Center of Quantum Matter, Beijing 100871, China*

(Dated: September 24, 2021)

We perform a lattice QCD calculation of the $\eta_c \rightarrow 2\gamma$ decay width using a model-independent method, which does not require the momentum extrapolation of the off-shell form factors. This method also provides a direct and simple way to examine the finite-volume effects. We perform the calculation using $N_f = 2$ twisted mass fermion action. A statistically significant excited-state effects are observed and treated by applying a multi-state fit. The effects of the fine-tuning of the charm quark mass are examined and confirmed to be fully under control. Finally, using three lattice spacings for the continuum extrapolation, we obtain the decay width $\Gamma_{\eta_c\gamma\gamma} = 6.57(15)_{\text{stat}}(8)_{\text{sys}}$ keV, raising a 3.6σ tension with the experimental value of $\Gamma_{\eta_c\gamma\gamma} = 5.15(35)$ keV quoted by Particle Data Group. We comment on the comparison between the theoretical predication and the experimental measurements.

INTRODUCTION

As a multi-scale system which can probe various regimes of quantum chromodynamics (QCD), heavy quarkonium presents an ideal laboratory for testing the interplay between perturbative and nonperturbative QCD [1]. In quarkonium physics the two-photon decay widths of quarkonium play an important role in connecting QCD from perturbative to nonperturbative regime. These quantities are traditionally expressed as the short-distance quark-antiquark annihilation decay rates multiplying the squared bound-state wave function at the origin [2]. Phenomenologically, the latter provides an essential, universal input for evaluating the decay and production cross sections for the quarkonium states [3].

In this study we focus on the two-photon decay of the lowest charmonium state, $\eta_c \rightarrow 2\gamma$, which has attracted extensive attentions from both experiments [4–21] and theories [2, 22–30]. On the experimental side, the mixing of η_c with other pseudo-scalars makes the accurate measurements of the two-photon decay extremely difficult. Despite the decades of effort, the experimental uncertainties of the decay width still range from 20% to 100%. The decay width $\Gamma_{\eta_c\gamma\gamma} = 5.15(35)$ keV quoted by Particle Data Group (PDG) is compiled using a combined fit with other decay channels. It results in a branching ratio of $\text{Br}(\eta_c \rightarrow 2\gamma) = (1.61 \pm 0.12) \times 10^{-4}$, denoted here as the “PDG-fit” value. If one examines the PDG list in details, there is another value of $\text{Br}(\eta_c \rightarrow 2\gamma) = 1.9_{-0.6}^{+0.7} \times 10^{-4}$ compiled based on the average of two latest experimental measurements [20, 21]. We denote it as the “PDG-aver” value. Note that PDG-fit value has a 5 times smaller uncertainty and a 15% lower central value compared to the PDG-aver one. Theoretically, a recent calculation based Dyson-Schwinger equation [23] yields a two-photon decay width $\Gamma_{\eta_c\gamma\gamma} = 6.32 \sim 6.39$ keV (with a branching ratio of $\text{Br}(\eta_c \rightarrow 2\gamma) = 1.98 \sim 2.00 \times 10^{-4}$), which is consistent with the PDG-aver value but much

larger than the PDG-fit one. Another study from non-relativistic QCD including the next-to-next-to-leading-order perturbative corrections [25] gives the branching ratio $\text{Br}(\eta_c \rightarrow 2\gamma) = 3.1 \sim 3.3 \times 10^{-4}$. This value is larger than other theoretical predictions and the experimental measurements. To clarify the discrepancies, it is important to have a first-principle calculation of $\eta_c \rightarrow 2\gamma$ decay width from lattice QCD.

The lattice QCD calculation of $\eta_c \rightarrow 2\gamma$ decay has been carried out before, but the systematic effects are not yet fully under control [28–30]. The aim of this work is to systematically scrutinize the lattice study of this radiative decay. Compared to the previous calculations, several improvements are made to obtain an accurate result. i) We adopt a novel method to extract the on-shell form factor straightforwardly, which avoids the conventional model-dependent errors caused by the momentum extrapolation of the off-shell form factors. ii) We perform a spatial volume integral to obtain the form factor, where a truncation range can be freely introduced to monitor the finite-volume effects. iii) We remove the excited-state contamination, which are found to be significant in this study but not fully addressed in the previous calculations. iv) We confirm that the systematic effects from the fine-tuning of the charm quark mass are smaller than the statistical errors. v) We perform a continuum extrapolation using three lattice spacings and find that the lattice results are well described by the fitting curves. The efforts to control various systematic effects finally allow us to obtain the decay width with a precision of 2.6%.

METHODOLOGY

We start the discussion of $H \rightarrow \gamma\gamma$ from an infinite-volume Euclidean system, where H indicates a hadron with the mass m_H . The relevant hadronic matrix element

$\mathcal{F}_{\mu\nu}(p)$ for the two-photon decay process is given by

$$\mathcal{F}_{\mu\nu}(p) = \int dt e^{m_H t/2} \int d^3\vec{x} e^{-i\vec{p}\cdot\vec{x}} \mathcal{H}_{\mu\nu}(t, \vec{x}), \quad (1)$$

where the hadronic function $\mathcal{H}_{\mu\nu}(t, \vec{x})$ is defined as

$$\mathcal{H}_{\mu\nu}(t, \vec{x}) = \langle 0 | T [J_\mu^{em}(x) J_\nu^{em}(0)] | H(k) \rangle, \quad (2)$$

with the initial state $|H(k)\rangle$ carrying the momentum $k = (im_H, \vec{0})$. The momentum assigned for the electromagnetic current $J_\mu^{em} = \sum_q e_q \bar{q} \gamma_\mu q$ ($e_q = 2/3, -1/3, -1/3, 2/3$ for $q = u, d, s, c$) takes the value of $p = (im_H/2, \vec{p})$ with $|\vec{p}| = m_H/2$. It satisfies the on-shell condition for the photon.

We then assume that the hadron in the initial state is a pseudo-scalar particle. According to its negative parity, the hadronic tensor $\mathcal{F}_{\mu\nu}(p)$ can be parameterized as

$$\mathcal{F}_{\mu\nu}(p) = \epsilon_{\mu\nu\alpha\beta} p_\alpha k_\beta F_{H\gamma\gamma}. \quad (3)$$

By multiplying $\epsilon_{\mu\nu\alpha\beta} p_\alpha k_\beta$ to both side, the form factor at on-shell momentum is extracted through

$$F_{H\gamma\gamma} = -\frac{1}{2m_H |\vec{p}|^2} \int d^4x e^{-ipx} \epsilon_{\mu\nu\alpha 0} \frac{\partial \mathcal{H}_{\mu\nu}(x)}{\partial x_\alpha}. \quad (4)$$

After averaging over the spatial direction for \vec{p} , $F_{H\gamma\gamma}$ would be obtained through

$$F_{H\gamma\gamma} = -\frac{1}{2m_H} \int d^4x e^{\frac{m_H}{2}t} \frac{j_1(|\vec{p}||\vec{x}|)}{|\vec{p}||\vec{x}|} \epsilon_{\mu\nu\alpha 0} x_\alpha \mathcal{H}_{\mu\nu}(x), \quad (5)$$

where $j_n(x)$ are the spherical Bessel functions. The decay width is then given by

$$\Gamma_{H\gamma\gamma} = \frac{\pi}{4} \alpha^2 m_H^3 F_{H\gamma\gamma}^2. \quad (6)$$

In the lattice calculation we adopt the infinite-volume reconstruction method proposed in Ref. [31]. This method has been successfully applied to various processes [32–39] to reconstruct the infinite-volume hadronic function using the finite-volume ones. In this work, we use it for the lattice calculation of $\eta_c \rightarrow 2\gamma$ decay. It is natural to introduce an integral truncation t_s in Eq. (5) and write the contribution as $F_{\eta_c\gamma\gamma}(t_s)$. The parameter t_s is chosen sufficiently large to guarantee that the time dependence of $\mathcal{H}_{\mu\nu}(t, \vec{x})$ for $t > t_s$ is dominated by the ground state, which is the J/ψ state when neglecting the disconnected diagrams. Then the residual integral from t_s to ∞ can be calculated as

$$\begin{aligned} \delta F_{\eta_c\gamma\gamma}(t_s) &= -\frac{1}{2m_{\eta_c}} \frac{e^{|\vec{p}|t_s}}{\sqrt{m_{J/\psi}^2 + |\vec{p}|^2 - |\vec{p}|^2}} \\ &\times \int d^3\vec{x} \frac{j_1(|\vec{p}||\vec{x}|)}{|\vec{p}||\vec{x}|} \epsilon_{\mu\nu\alpha 0} x_\alpha \mathcal{H}_{\mu\nu}(t_s, \vec{x}). \end{aligned} \quad (7)$$

The total contribution of $F_{\eta_c\gamma\gamma}$ is given by

$$F_{\eta_c\gamma\gamma} = F_{\eta_c\gamma\gamma}(t_s) + \delta F_{\eta_c\gamma\gamma}(t_s), \quad (8)$$

where the t_s dependence cancels if ground-state saturation is satisfied. We then use the hadronic function $\mathcal{H}_{\mu\nu}^L(t, \vec{x})$ calculated on a finite-volume lattice to replace the infinite-volume $\mathcal{H}_{\mu\nu}(t, \vec{x})$ for $t \leq t_s$. Such replacement only amounts for an exponentially suppressed finite-volume effects as the hadronic function $\mathcal{H}_{\mu\nu}(t, \vec{x})$ itself suppresses exponentially when $|\vec{x}|$ becomes large. One can introduce a spatial integral truncation R and examine at large R whether the finite-volume effects are well under control or not.

The method used in our calculation is generically different from the traditional approach where the photon momenta are assigned by discrete Fourier transformation and the off-shell form factors [28] or amplitude squares [30] with nonzero photon virtualities are calculated. In that case, the physical results can only be obtained after a continuous momentum extrapolation to the on-shell limit. The situation becomes much easier here as the approach presented above allows us to extract the on-shell form factor straightforwardly, without calculating various off-shell form factors and carrying out the momentum extrapolation. Therefore, the systematic uncertainty from the model-dependent extrapolation is avoided and the computational cost is also significantly reduced.

NUMERICAL SETUP

Ensemble	a (fm)	$L^3 \times T$	$N_{\text{conf}} \times T$	$a\mu$	m_π (MeV)	Δt
a98	0.098	$24^3 \times 48$	236×48	0.006	365	7-16
a85	0.085	$24^3 \times 48$	200×48	0.004	315	8-19
a67	0.0667	$32^3 \times 64$	197×64	0.003	300	10-24

Table I. Parameters of gauge ensembles used in this work. From left to right, we list the ensemble name, the lattice spacing a , the spatial and temporal lattice size L and T , the number of the measurements of the correlation function for each ensemble $N_{\text{conf}} \times T$ with N_{conf} the number of the configurations used, the light quark mass $a\mu$, the pion mass m_π and the range of the time separation Δt . Here, L , T and Δt are given in lattice units. For all ensembles, Δt takes a consistent range of 0.7-1.6 fm.

The calculation is performed using three $N_f = 2$ -flavor twisted mass gauge field ensembles generated by the Extended Twisted Mass Collaboration (ETMC) [40] with lattice spacing $a \simeq 0.0667, 0.085, 0.098$ fm. The ensemble parameters are given in Table. I. The valence charm quark mass is tuned by making the lattice result of 1) the mass of η_c or 2) the mass of J/ψ approach to its physical value. For simplicity, we add the suffix “-P” and “-IP” to the ensemble name to specify the cases of 1) and 2). For the detailed information of the tuning, we refer to the supplemental material.

In this work, we calculate the three-point correlation function $C_{\mu\nu}^{(3)}(x, y, t_i) \equiv \langle J_\mu^{em}(x) J_\nu^{em}(y) \mathcal{O}_{\eta_c}^\dagger(t_i) \rangle$ with $t_i = \min\{t_x, t_y\} - \Delta t$. The Z_4 -stochastic wall source propagator is placed at time t_i so that the $\mathcal{O}_{\eta_c}^\dagger$ operator carries the zero momentum. It is found in our study that the uncertainty is reduced by nearly a factor of 2 by using stochastic propagator compared to that using the point source propagator. We also find that the excited-state contamination associated with the $\mathcal{O}_{\eta_c}^\dagger$ operator is significant. We thus apply the APE [41] and Gaussian smearing [42] to the η_c field and it efficiently reduces the excited-state effects. Nevertheless, when the precision reaches 1-3% in our calculation the excited-state effects are statistically significant unless $\Delta t \gtrsim 1.6$ fm. Such systematic effects affect both two-point correlation function $C^{(2)}(t) = \langle \mathcal{O}_{\eta_c}(t) \mathcal{O}_{\eta_c}^\dagger(0) \rangle$ and three-point function $C_{\mu\nu}^{(3)}$. Using a two-state fit form, we write the time dependence for $C^{(2)}(t)$ as

$$C^{(2)}(t) = V \sum_{i=0,1} \frac{Z_i^2}{2E_i} \left(e^{-E_i t} + e^{-E_i(T-t)} \right) \quad (9)$$

with V the spatial-volume factor, $E_0 = m_{\eta_c}$ the ground-state energy and E_1 the energy for the first excited state. $Z_i = \frac{1}{\sqrt{V}} \langle i | \mathcal{O}_{\eta_c}^\dagger | 0 \rangle$ ($i = 0, 1$) are the overlap amplitudes for the ground and the first excited state. We then use Z_0 and m_{η_c} as the inputs to determine the hadronic function $\mathcal{H}_{\mu\nu}$ through $\mathcal{H}_{\mu\nu}(t_x - t_y, \vec{x} - \vec{y}) = C_{\mu\nu}^{(3)}(x, y, t_i) / [(Z_0/2m_{\eta_c})e^{-m_{\eta_c}(t_y-t_i)}]$. The excited-state effects carried by $\mathcal{H}_{\mu\nu}$ propagate into the form factor $F_{\eta_c\gamma\gamma}$ and can be parameterized using a relatively simple two-state form

$$F_{\eta_c\gamma\gamma}(\Delta t) = F_{\eta_c\gamma\gamma} + \xi e^{-(E_1-E_0)\Delta t}, \quad (10)$$

with two unknown parameters $F_{\eta_c\gamma\gamma}$ and ξ . To fully control the systematic effects, we use various Δt from the range of 0.7 - 1.6 fm and fit the lattice data to the form (10). To compute the correlation function for the whole set of $\vec{x} - \vec{y}$, we place the point source propagator on one vector current and treat the other one as the sink. Both the point and the stochastic wall source propagators are placed on all time slices and thus the average based on time translation invariance can be performed to increase the statistics.

In our calculation the electromagnetic current is replaced by a local charm quark current as $J_\mu^{em}(x) = Z_V e_c J_\mu^{(c)}(x)$ with $J_\mu^{(c)}$ defined as $J_\mu^{(c)} \equiv \bar{c}\gamma_\mu c$. Here Z_V is a renormalization factor, which converts the local vector current to the conserved one. For the details of the determination of Z_V we refer to the supplemental material.

LATTICE RESULTS

The lattice results of $F_{\eta_c\gamma\gamma}$ as a function of the truncation time t_s with different separations Δt are shown

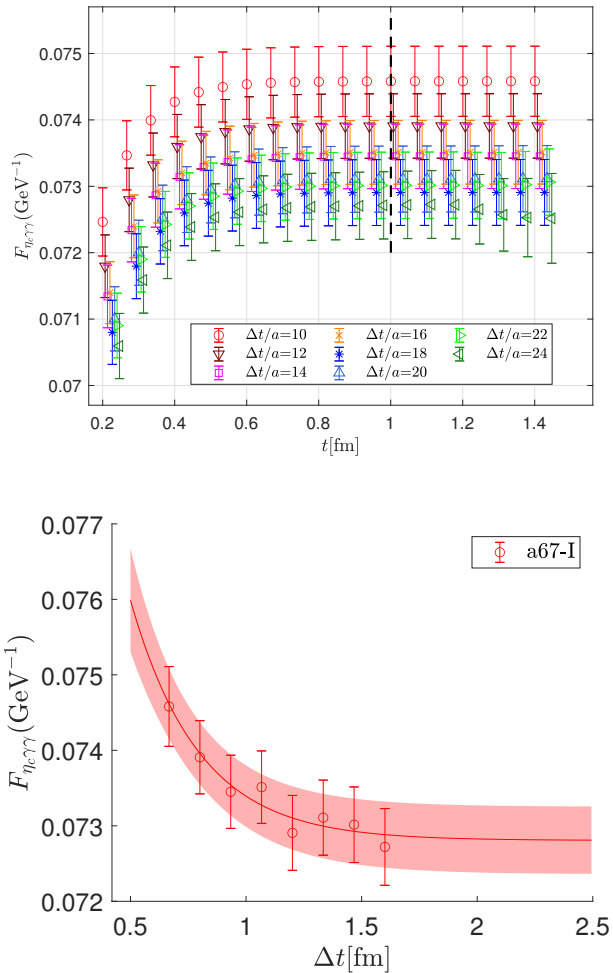


Figure 1. The lattice results of $F_{\eta_c\gamma\gamma}$ for ensemble a67-I. On the top panel, $F_{\eta_c\gamma\gamma}$ are shown as a function of t_s with various choices of Δt . The dashed line denotes a conservative choice of $t_s \simeq 1$ fm, where the ground-state saturation is satisfied. On the bottom panel, $F_{\eta_c\gamma\gamma}$ with $t_s \simeq 1$ fm are shown as a function of Δt together with a fit to the form (10).

on the top panel in Fig. 1. Here we take the ensemble with the finest lattice spacing, a67, as an example. The results are shown with the charm quark mass tuned to the physical point $m_{\eta_c} \simeq m_{\eta_c}^{\text{phys}}$. The integral in Eq. (5) is performed with \vec{x} summed over the whole spatial volume. We find that for all the separation Δt and all ensembles used in this work, a temporal truncation $t_s \simeq 1$ fm is a conservative choice for the ground-state saturation. With this choice, the results for $F_{\eta_c\gamma\gamma}$ as a function of Δt are shown on the bottom panel in Fig. 1. It shows that $F_{\eta_c\gamma\gamma}$ has an obvious Δt dependence, indicating the sizable excited-state effects associated with $\mathcal{O}_{\eta_c}^\dagger$ operator as we have pointed out before. Using a two-state fit described by Eq. (10) we extract the ground-state contribution to the form factor at $\Delta t \rightarrow \infty$.

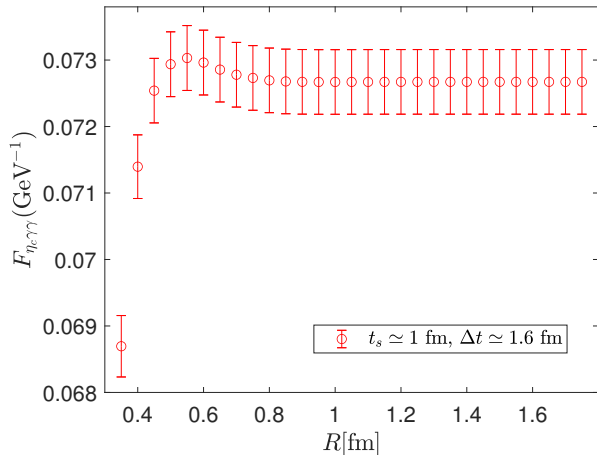


Figure 2. For ensemble a67-I, $F_{\eta_c \gamma \gamma}$ with $t_s \simeq 1$ fm and $\Delta t \simeq 1.6$ fm as a function of the spatial range truncation R .

To examine the finite-volume effects, we introduce a spatial integral truncation R in both Eqs. (5) and (7). As the hadronic function $\mathcal{H}_{\mu\nu}(x)$ is dominated by the J/ψ state at large $|\vec{x}|$, the size of the integrand exponentially suppresses when $|\vec{x}|$ becomes large. In Fig. 2 the form factor $F_{\eta_c \gamma \gamma}$ is shown as a function of R . For $R \gtrsim 0.8$ fm, there exists a plateau, indicating that the hadronic function $\mathcal{H}_{\mu\nu}(x)$ at $|\vec{x}| \gtrsim 0.8$ fm has negligible contribution to $F_{\eta_c \gamma \gamma}$. For each of the three ensembles used here, the lattice size satisfies $L > 2$ fm, sufficiently large to accommodate the hadronic system. We thus conclude the finite-volume effects are well under control in our calculation. Here the parameter R is simply introduced for the examination of the size of the finite-volume effects, while the lattice results reported throughout the paper are compiled based on the whole spatial-volume summation.

Ensemble	a98-I	a85-I	a67-I
$\Gamma_{\eta_c \gamma \gamma}$ (keV)	5.19(18)	5.59(8)	5.91(7)
Ensemble	a98-II	a85-II	a67-II
$\Gamma_{\eta_c \gamma \gamma}$ (keV)	5.22(16)	5.60(8)	5.96(6)

Table II. Decay width for all three ensembles.

Using the form factor as an input, the decay width $\Gamma_{\eta_c \gamma \gamma}$ is evaluated and listed in Table II. The lattice results of $\Gamma_{\eta_c \gamma \gamma}$ as a function of lattice spacing a are shown in Fig. 3 together with a linear fit in a^2 . The fitting curves describe the lattice data well. After the continuum extrapolation, the results for $\Gamma_{\eta_c \gamma \gamma}$ are obtained as

$$\Gamma_{\eta_c \gamma \gamma} = \begin{cases} 6.49(19) \text{ keV} & \text{set } \mu_c \text{ by } \eta_c \\ 6.57(15) \text{ keV} & \text{set } \mu_c \text{ by } J/\psi \end{cases}. \quad (11)$$

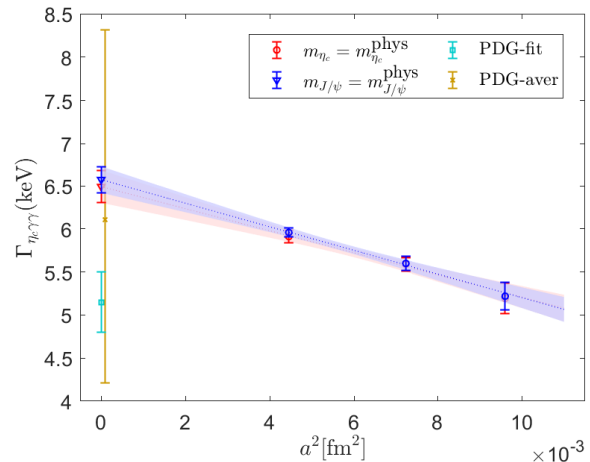


Figure 3. The lattice results of the decay width of $\Gamma_{\eta_c \gamma \gamma}$ as a function of the lattice spacing. The symbol of red circle and blue triangle denote the lattice results from ensemble-I and -II, respectively. The symbol of cyan square and orange cross indicate the PDG-fit and PDG-aver values. Here PDG-aver data point is shifted horizontally to favor a clear comparison.

A good consistency of $\Gamma_{\eta_c \gamma \gamma}$ is observed under the variation of the charm quark mass. Finally we report the result of the decay width as

$$\Gamma_{\eta_c \gamma \gamma} = 6.57(15)_{\text{stat}}(8)_{\text{sys}} \text{ keV}, \quad (12)$$

where the decay width calculated at $m_{J/\psi} \approx m_{J/\psi}^{\text{phys}}$ is quoted as the central value and the deviation shown in Eq. (11) is treated as a systematic uncertainty. Our lattice result is larger than the PDG-fit value by 28% with a 3.6- σ deviation, but compatible with PDG-aver value as it carries a large uncertainty. The two PDG values are also printed in Fig. 3 for a comparison.

DISCUSSION

The PDG-aver value $\text{Br}(\eta_c \rightarrow 2\gamma) = 1.9_{-0.6}^{+0.7} \times 10^{-4}$ is taken from an average of BESIII [20] and CLEO [21] measurements, with $\text{Br}(\eta_c \rightarrow 2\gamma) = 2.7 \pm 0.8 \pm 0.6 \times 10^{-4}$ and $\text{Br}(\eta_c \rightarrow 2\gamma) = 1.4_{-0.5}^{+0.7} \pm 0.3 \times 10^{-4}$, respectively. These results are rather far apart from each other, but still consistent due to large errors. Such large errors propagate into the PDG-aver value and cause a 32-37% uncertainty there. As for the PDG-fit value, other decay channels are also used. The constraints from different η_c decays result in a much smaller error and a downward shift of the central value. The significantly suppressed uncertainty in the PDG-fit value indicates that the direct experimental measurements of the $\eta_c \rightarrow 2\gamma$ decay have little impact here. The fit relies on the assumption that all individual measurements are correctly statistically distributed

and the correlations among the different decay modes are explicitly known. This is relatively difficult and the assumption may not be valid for all the measurements. According to the table of the correlation coefficients used in the PDG fit, it exists a large correlation between the $\eta_c \rightarrow 2\gamma$ decay and other decay modes, indicating that the PDG-fit result is easily affected by the parametrization in the constrained fit. Thus a direct and precise experimental measurement of $\eta_c \rightarrow 2\gamma$ is essential for our better understanding of the charmonium radiative decays.

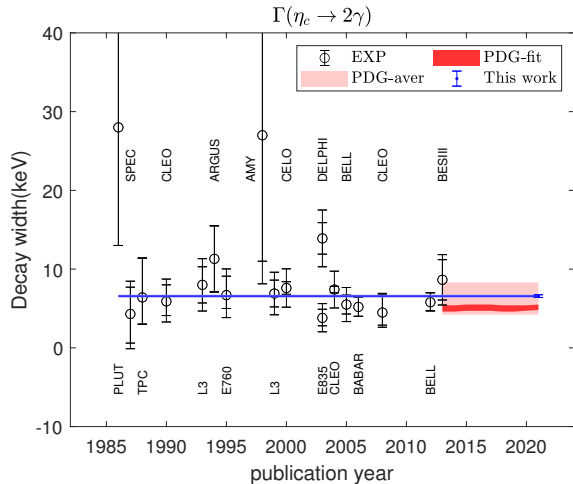


Figure 4. The historical perspective of the decay width $\Gamma(\eta_c \rightarrow 2\gamma)$ from various experiments. Since 2013, PDG starts to produce the average and fit results using BESIII (2013) and CLEO (2008) data as inputs. The lattice result, PDG-aver and PDG-fit results are represented by the blue point, light band and deep band, respectively.

In Fig. 4 we summarize the experimental measurements of $\Gamma_{\eta_c\gamma\gamma}$ from 1986 to 2013 [4–21]. These results are very consistent with our lattice calculation but carry quite large errors, which range from 20% to 100%. It is still challenging to reduce the uncertainty to the level of few percent. Regarding this situation, for a certain period of time the first-principle determination of $\Gamma_{\eta_c\gamma\gamma}$ from lattice QCD will play an irreplaceable role in a better understanding of the QCD dynamics in charmonium physics.

The systematic error budget in our lattice calculation is relatively complete. The remaining systematic effects requiring further investigation are the neglected disconnected diagrams, the quenching of strange quark and the use of up and down quarks heavier than their physical values in our calculation. The first effect is Okubo-Zweig-Iizuka (OZI) suppressed and believed to only gives a small contribution in the charmonium system [43–46]. For the other two, previous lattice calculations [47] indicate that they will also result in only small effects. Thus,

none of them are expected to explain the 28% discrepancy between our lattice result and the PDG-fit value.

CONCLUSION

In this work we adopt a new method to compute the decay width of $\eta_c \rightarrow 2\gamma$, where the on-shell form factor is obtained by combining the hadronic function calculated from lattice QCD and an appropriate weight function known analytically. As this method does not require the model description of the momentum dependence of the form factor, it provides a theoretically clean framework to determine the radiative decay width. Such method can also be applied for other processes which involve the leptonic or radiative particles in the final states, for example $\pi^0 \rightarrow 2\gamma$ [48, 49], $J/\psi \rightarrow 3\gamma$ [50], $\pi \rightarrow e^+e^-$ [51], $K_L \rightarrow \mu^+\mu^-$ [52] and radiative leptonic decays $K^- \rightarrow \ell^-\bar{\nu}\gamma$, $D_s^+ \rightarrow \ell^+\nu\gamma$, $B \rightarrow \ell^-\bar{\nu}\gamma$ [53, 54].

Our lattice result for the decay width is consistent with most of the previous experimental measurements and also the PDG-aver value, but notably different from the PDG-fit value by 3.6 standard deviations. We suspect that the error of the PDG-fit value might be underestimated due to the limited knowledge on the direct experimental measurements of $\eta_c \rightarrow 2\gamma$. It is crucial for the forthcoming experiments, e.g. BESIII, to further reduce the experimental uncertainties. The cross check of our results by other lattice QCD calculations are also very helpful to clarify the discrepancy between theory and experiments.

We thank ETM Collaboration for sharing the gauge configurations with us. A particular acknowledgement goes to Carsten Urbach. We gratefully acknowledge many helpful discussions with Michael Doser, Luchang Jin, Haibo Li and Yan-Qing Ma. Y.M. acknowledges support by NSFC of China under Grant No. 12047505 and State Key Laboratory of Nuclear Physics and Technology, Peking University. X.F. and T.W. were supported in part by NSFC of China under Grant No. 11775002, 12125501 and National Key Research and Development Program of China under Contracts No. 2020YFA0406400. X.F., C.L. and Z.H.Z. are supported in part by NSFC of China under Grant No. 12070131001. C.L. and Z.H.Z. are also supported in part by CAS Interdisciplinary Innovation Team and NSFC of China under Grant No. 11935017. The main calculation was carried out on Tianhe-1A supercomputer at Tianjin National Supercomputing Center and partly supported by High-performance Computing Platform of Peking University.

-
- [1] N. Brambilla *et al.*, *Eur. Phys. J. C* **71**, 1534 (2011), 1010.5827.
 - [2] G. T. Bodwin, E. Braaten, and G. P. Lepage, *Phys.*

- Rev. D **51**, 1125 (1995), hep-ph/9407339, [Erratum: Phys.Rev.D 55, 5853 (1997)].
- [3] E. J. Eichten and C. Quigg, Phys. Rev. D **52**, 1726 (1995), hep-ph/9503356.
- [4] PLUTO, C. Berger *et al.*, Phys. Lett. B **167**, 120 (1986).
- [5] Annecy(LAPP)-CERN-Genoa-Lyon-Oslo-Rome-Strasbourg-Turin, C. Baglin *et al.*, Phys. Lett. B **187**, 191 (1987).
- [6] TPC/Two Gamma, H. Aihara *et al.*, Phys. Rev. Lett. **60**, 2355 (1988).
- [7] CLEO, W. Y. Chen *et al.*, Phys. Lett. B **243**, 169 (1990).
- [8] L3, O. Adriani *et al.*, Phys. Lett. B **318**, 575 (1993).
- [9] ARGUS, H. Albrecht *et al.*, Phys. Lett. B **338**, 390 (1994).
- [10] E760, T. A. Armstrong *et al.*, Phys. Rev. D **52**, 4839 (1995).
- [11] AMY, M. Shirai *et al.*, Phys. Lett. B **424**, 405 (1998).
- [12] L3, M. Acciarri *et al.*, Phys. Lett. B **461**, 155 (1999), hep-ex/9909008.
- [13] CLEO, G. Brandenburg *et al.*, Phys. Rev. Lett. **85**, 3095 (2000), hep-ex/0006026.
- [14] Fermilab E835, M. Ambrogiani *et al.*, Phys. Lett. B **566**, 45 (2003).
- [15] DELPHI, J. Abdallah *et al.*, Eur. Phys. J. C **31**, 481 (2003), hep-ex/0311002.
- [16] CLEO, D. M. Asner *et al.*, Phys. Rev. Lett. **92**, 142001 (2004), hep-ex/0312058.
- [17] Belle, C. C. Kuo *et al.*, Phys. Lett. B **621**, 41 (2005), hep-ex/0503006.
- [18] BaBar, B. Aubert *et al.*, Phys. Rev. Lett. **96**, 052002 (2006), hep-ex/0510070.
- [19] Belle, C. C. Zhang *et al.*, Phys. Rev. D **86**, 052002 (2012), 1206.5087.
- [20] BESIII, M. Ablikim *et al.*, Phys. Rev. D **87**, 032003 (2013), 1208.1461.
- [21] CLEO, G. S. Adams *et al.*, Phys. Rev. Lett. **101**, 101801 (2008), 0806.0671.
- [22] S. Godfrey and N. Isgur, Phys. Rev. D **32**, 189 (1985).
- [23] J. Chen, M. Ding, L. Chang, and Y.-x. Liu, Phys. Rev. D **95**, 016010 (2017), 1611.05960.
- [24] F. Feng, Y. Jia, and W.-L. Sang, Phys. Rev. Lett. **115**, 222001 (2015), 1505.02665.
- [25] F. Feng, Y. Jia, and W.-L. Sang, Phys. Rev. Lett. **119**, 252001 (2017), 1707.05758.
- [26] R. Li, Y. Feng, and Y.-Q. Ma, JHEP **05**, 009 (2020), 1911.05886.
- [27] R. Zhang *et al.*, (2021), 2107.12749.
- [28] J. J. Dudek and R. G. Edwards, Phys. Rev. Lett. **97**, 172001 (2006), hep-ph/0607140.
- [29] CLQCD, T. Chen *et al.*, Eur. Phys. J. C **76**, 358 (2016), 1602.00076.
- [30] C. Liu, Y. Meng, and K.-L. Zhang, Phys. Rev. D **102**, 034502 (2020), 2004.03907.
- [31] X. Feng and L. Jin, Phys. Rev. D **100**, 094509 (2019), 1812.09817.
- [32] X.-Y. Tuo, X. Feng, and L.-C. Jin, Phys. Rev. D **100**, 094511 (2019), 1909.13525.
- [33] X. Feng, Y. Fu, and L.-C. Jin, Phys. Rev. D **101**, 051502 (2020), 1911.04064.
- [34] X. Feng, M. Gorchtein, L.-C. Jin, P.-X. Ma, and C.-Y. Seng, Phys. Rev. Lett. **124**, 192002 (2020), 2003.09798.
- [35] N. H. Christ, X. Feng, J. Lu-Chang, and C. T. Sachrajda, PoS **LATTICE2019**, 259 (2020).
- [36] N. H. Christ, X. Feng, L.-C. Jin, and C. T. Sachrajda, Phys. Rev. D **103**, 014507 (2021), 2009.08287.
- [37] P.-X. Ma, X. Feng, M. Gorchtein, L.-C. Jin, and C.-Y. Seng, Phys. Rev. D **103**, 114503 (2021), 2102.12048.
- [38] X.-Y. Tuo, X. Feng, L.-C. Jin, and T. Wang, (2021), 2103.11331.
- [39] X. Feng, L. Jin, and M. J. Riberdy, (2021), 2108.05311.
- [40] ETM, P. Boucaud *et al.*, Comput. Phys. Commun. **179**, 695 (2008), 0803.0224.
- [41] APE, M. Albanese *et al.*, Phys. Lett. B **192**, 163 (1987).
- [42] S. Gusken, Nucl. Phys. B Proc. Suppl. **17**, 361 (1990).
- [43] UKQCD, C. McNeile and C. Michael, Phys. Rev. D **70**, 034506 (2004), hep-lat/0402012.
- [44] QCD-TARO, P. de Forcrand *et al.*, JHEP **08**, 004 (2004), hep-lat/0404016.
- [45] L. Levkova and C. DeTar, Phys. Rev. D **83**, 074504 (2011), 1012.1837.
- [46] HPQCD, D. Hatton *et al.*, Phys. Rev. D **102**, 054511 (2020), 2005.01845.
- [47] G. Bali *et al.*, PoS **LATTICE2011**, 135 (2011), 1108.6147.
- [48] X. Feng *et al.*, Phys. Rev. Lett. **109**, 182001 (2012), 1206.1375.
- [49] A. Gérardin, H. B. Meyer, and A. Nyffeler, Phys. Rev. D **94**, 074507 (2016), 1607.08174.
- [50] Y. Meng, C. Liu, and K.-L. Zhang, Phys. Rev. D **102**, 054506 (2020), 1910.11597.
- [51] N. H. Christ, X. Feng, L. Jin, C. Tu, and Y. Zhao, PoS **LATTICE2019**, 097 (2020), 2001.05642.
- [52] N. H. Christ, X. Feng, L. Jin, C. Tu, and Y. Zhao, PoS **LATTICE2019**, 128 (2020).
- [53] C. Kane, C. Lehner, S. Meinel, and A. Soni, PoS **LATTICE2019**, 134 (2019), 1907.00279.
- [54] A. Desiderio *et al.*, Phys. Rev. D **103**, 014502 (2021), 2006.05358.

SUPPLEMENTARY MATERIAL

In this section, we expand on a selection of technical details and add results to facilitate cross-checks of different calculations of the $\eta_c \rightarrow 2\gamma$ decay width.

Tuning of charm quark mass

The detailed information of the charm quark mass tuning is given in Table SI. We use the suffix “-I” and “-II” to distinguish the cases with $m_{\eta_c} \simeq m_{\eta_c}^{\text{phys}}$ and $m_{J/\psi} \simeq m_{J/\psi}^{\text{phys}}$. Together with the charmonium masses, we also list the values of the hyperfine splitting $\delta m \equiv m_{J/\psi} - m_{\eta_c}$. In the continuum limit (see Fig. 5), we obtain $\delta m = 123(1)$ MeV, which is 10 MeV larger than the PDG value. Similar increase of the hyperfine splitting has been observed by HPQCD collaboration [46], where the discarded η_c annihilation effects are expected to cause a 7.3(1.2) MeV enhancement in δm . In our calculation, the shift in δm could lead to a $\sim 0.3\%$ uncertainty in the η_c mass.

Ensemble	$a\mu_c$	m_{η_c} (MeV)	$m_{J/\psi}$ (MeV)	δm (MeV)
a98-I	0.2896	2984.9(4)	3064.8(5)	78.9(4)
a85-I	0.2563	2988.6(5)	3078.0(7)	89.4(5)
a67-I	0.2024	2987.6(5)	3090.4(7)	102.6(5)
a98-II	0.2951	3018.9(4)	3097.2(5)	78.4(3)
a85-II	0.2586	3005.7(5)	3094.4(7)	88.8(5)
a67-II	0.2036	2999.5(5)	3101.7(7)	102.3(5)
PDG		2983.9(4)	3096.9(0)	113.0(4)

Table SI. Tuning of the bare charm quark mass μ_c . The mass μ_c is tuned such that the mass of η_c or J/ψ approaches to its physical value, with the deviation controlled to be less than 0.2%. To distinguish the cases with $m_{\eta_c} \simeq m_{\eta_c}^{\text{phys}}$ and $m_{J/\psi} \simeq m_{J/\psi}^{\text{phys}}$, we add the suffix “-I” and “-II” to the ensemble name. $\delta m \equiv m_{J/\psi} - m_{\eta_c}$ is the hyperfine splitting.

Determination of Z_V

In our calculation the electromagnetic current is replaced by a local charm quark current as $J_\mu^{em}(x) = Z_V e_c J_\mu^{(c)}(x)$ with $J_\mu^{(c)}$ defined as $J_\mu^{(c)} \equiv \bar{c}\gamma_\mu c$. Here Z_V is

a vector-current renormalization factor, which can be calculated by applying the condition of charge conservation and using a ratio between $C^{(2)}(t)$ and the three-point function $C^{(3)}(t) = \sum_{\vec{x}} \langle \mathcal{O}_{\eta_c}(t) J_0^{(c)}(t/2, \vec{x}) \mathcal{O}_{\eta_c}^\dagger(0) \rangle$ with zero three-momentum inserted for both initial and final states. As the charge conservation holds for both ground and excited-states, we find that the excited-state effects in $C^{(3)}(t)$ and $C^{(2)}(t)$ cancel efficiently. The plateau of

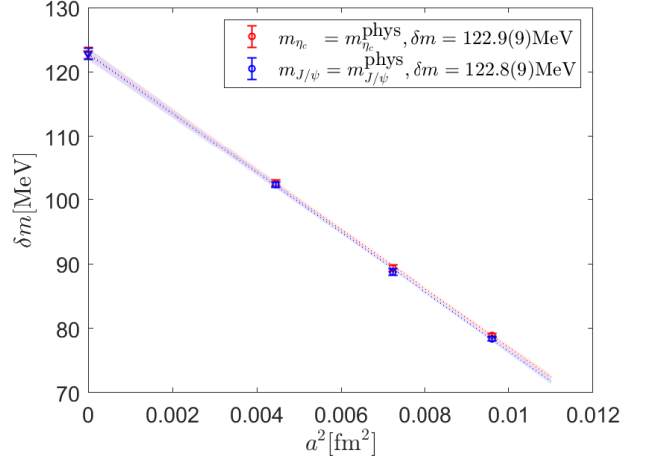


Figure 5. The continuum extrapolation of hyperfine splitting.

the ratio starts at $t \approx 1$ fm. The main systematic effect appears as the around-of-world effect in $C^{(2)}(t)$ at $t \approx T/2$. To account for this effect, we use the following relation

$$Z_V = \frac{C^{(2)}(t)}{C^{(3)}(t)} \frac{1}{(1 + e^{-m_{\eta_c}(T-2t)})}, \quad \text{for } t \lesssim T/2, \quad (\text{S1})$$

to extract Z_V from the ratio. We find that the uncertainty in the determination of the charm quark mass makes a nearly negligible impact on Z_V , whose numerical values are listed in Table SII.

Ensemble	a98-I	a85-I	a67-I
Z_V	0.6057(49)	0.6304(16)	0.6523(10)
Ensemble	a98-II	a85-II	a67-II
Z_V	0.6071(51)	0.6305(19)	0.6521(12)

Table SII. The vector-current renormalization constants Z_V calculated using Eq. (S1).